Available online at www.sciencedirect.com
SCIENCE DIRECT
Virology 349 (2006) 440–452
VIROLOGY
www.elsevier.com/locate/yviro

Correlation between SIV Tat evolution and AIDS progression in cerebrospinal fluid of morphine-dependent and control macaques infected with SIV and SHIV

Richard J. Noel Jr. [a,b,*], Ziomara Marrero-Otero [b], Rakesh Kumar [a,c], Gladys S. Chompre-González [b], Ashish S. Verma [a,c], Anil Kumar [a,c]

[a] *AIDS Research Program, Ponce School of Medicine, Ponce, PR 00732, USA*
[b] *Department of Biochemistry, Ponce School of Medicine, Ponce, PR 00732, USA*
[c] *Laboratory of Viral Immunology, Department of Microbiology, Ponce School of Medicine, Ponce, PR 00732, USA*

Received 16 November 2005; returned to author for revision 21 February 2006; accepted 18 March 2006
Available online 27 April 2006

Abstract

Morphine abuse has been associated with higher virus replication and accelerated disease progression in a non-human primate model of AIDS. In our previous report, we have shown that 50% of morphine-addicted macaques progress rapidly and that 2/3 of the rapid progressors exhibit severe neuropathogenesis. In this report, we examined the sequence evolution of the SIV Tat protein, known to participate in AIDS neuropathology, in the cerebrospinal fluid (CSF) of morphine-dependent and control macaques over the first 20 weeks of infection. The CSF SIV Tat evolution was found to be inversely related with disease progression, and the highly neuropathogenic inoculum clone sequence was the prevalent CSF form in rapid progressors. Divergence from the inoculum clone was significantly greater in both morphine-dependent normal progressors and control macaques than in the morphine-dependent rapid progressors. Furthermore, we also found evidence of a trend that morphine alters the type of mutation, resulting in an enhanced ratio of transitions to transversions (Ts:Tv). Rapid disease exacerbates this trend and appears to influence the distribution of nonsynonymous changes in the first exon of SIV *tat*, with a clear majority of mutations occurring in the C-terminal half of the protein where the known functionally important domains reside. Thus, morphine abuse may change the nature and extent of mutations that drive viral evolution.

Keywords: SIV; SHIV; AIDS; Macaque; Morphine; Tat evolution; Cerebrospinal fluid

Introduction

The human immunodeficiency virus (HIV-1) is a member of a subfamily of neurotropic viruses called the Lentivirinae (Gonda et al., 1985). The entry of HIV-1 into the brain occurs shortly after the host is infected and has been widely detected in the central nervous system (CNS) by a variety of techniques (Davis et al., 1992; Gabuzda et al., 1986; Gartner et al., 1986; Stoler et al., 1986). The clinical consequences of HIV-1 infection of the CNS are varied and depend on both host and viral factors in a manner that remains very actively studied. Acute neuropathologies such as ataxia and meningitis are relatively common and intermittent (Hollander and Stringari, 1987; Scarpini et al., 1991). More severe forms of HIV-1-associated neuropathology include HIV-1 encephalitis and HIV-1-associated dementia (HIVD), but are less frequent, occurring in 10–20% of HIV-infected persons; and this rate may be declining with the use of increasingly effective antiretroviral treatment (Navia et al., 1986a, 1986b; Tozzi et al., 2005; Maschke et al., 2000; Neuenburg et al., 2002; McCoig et al., 2002). Typically, HIVD is a sub-cortical dementia characterized by cognitive, behavioral and motor abnormalities (Navia et al., 1986a, 1986b), although the clinical manifestation in the HAART era has altered somewhat in pattern, representing

* Corresponding author. AIDS Research Program, Ponce School of Medicine, Ponce, PR 00732-7004, USA. Fax: +1 787 841 1040.
E-mail address: rnoel@psm.edu (R.J. Noel).

0042-6822/$ - see front matter © 2006 Elsevier Inc. All rights reserved.
doi:10.1016/j.virol.2006.03.032

greater cortical involvement (Cysique et al., 2004). To date, there have been few clear correlations between viral infection and the development of severe neuropathology associated with HIV-1 infection. Viral load in the plasma or CSF or particular viral characteristics, beyond macrophage tropism, have not proven reproducibly associated with HIVD. Rather, infiltration of infected macrophages and the presence of multinucleated giant cells in the brain have been strongly linked to severe neuropathology (Anderson et al., 2002; Gonzalez et al., 2002; Ryan et al., 2002; Gartner et al., 1986). Although the cause–effect relationship between macrophage infiltration and HIVD remains unclear mechanistically, a wide number of reports have suggested specific roles for viral proteins and host factors including genetics and lifestyle (Corder et al., 1998; Gonzalez et al., 2002; Bell et al., 1998; Tozzi et al., 2005). Among the clearest of behavioral correlates, HIV neuropathology has been reported with increased frequency in the context of drug abuse (Donahoe and Falek, 1988; Nath et al., 2002; Bell et al., 1998; Zhang et al., 1998).

The mechanism by which drug abuse contributes to HIV infection and pathogenesis, including neuropathogenesis, is not completely clear, although it represents a considerable problem for both science and society. Nearly 30% of the AIDS cases reported in the US include injection drug abuse as a risk factor (Purcell et al., 2004). Drug abuse itself portends a variety of risk behaviors that assist in the spread of infection, yet there are also cellular and biochemical changes caused by drugs of abuse that may contribute to viral pathogenesis. Heroin, an opiate that is converted to morphine for biological activity is a major injected drug of abuse. Opiate drugs have controversial effects on HIV infection and progression to AIDS, with some studies reporting enhanced pathogenesis and others indicating a possible survival advantage of morphine use (Chuang et al., 2005; Kumar et al., 2004; Donahoe, 2004; Kapadia et al., 2005). However, at the cellular level, opiates have been reported to increase viral replication rate and rate of infection of monocytes, upregulate chemokines and receptors and upregulate viral gene expression (Peterson et al., 1990; Chuang et al., 1993, 2005; Kumar et al., 2004; Li et al., 2003; Squinto et al., 1990; Peterson et al., 1994, 2004; Steele et al., 2003). More specifically, with respect to HIV neuropathogenesis, opiates change the gene expression of cells in the brain causing altered gene regulation of host cytokines, cytokine receptors as well as the mu opioid receptor (El Hage et al., 2006; Chang et al., 1996; Steele et al., 2003; Yu et al., 2003). Furthermore, recent reports have indicated that opiates have synergistic effects on glial cells in conjunction with viral proteins, such as the viral transactivator Tat (Gurwell et al., 2001; Nath et al., 2002; Turchan et al., 2001).

The Tat protein of primate lentiviruses has been widely implicated as a critical viral protein in the development of neuropathogenesis during infection (Hudson et al., 2000). Tat can be produced and secreted from infected cells and taken up by surrounding uninfected cells (Chang et al., 1997; Ensoli et al., 1993; Ma and Nath, 1997). Thus, even though neurons are not infected by HIV-1, soluble Tat can directly cause neuronal apoptosis (Jones et al., 1998; New et al., 1997). Furthermore, Tat has been implicated as an indirect mediator of neuropathology by its effects on other brain cells. Tat can alter gene expression in both astrocytes and microglia, including cytokines, chemokines, iNOS and adhesion molecules (Pu et al., 2003; Woodman et al., 1999; Abraham et al., 2003; Chauhan et al., 2003; Conant et al., 1996; Koller et al., 2001; Kutsch et al., 2000; Liu et al., 2002; McManus et al., 2000; Nicolini et al., 2001; Polazzi et al., 1999). In in vivo models, the expression or application of Tat in the brain causes changes consistent with the development of HIVD (Jones et al., 1998; Kim et al., 2003). Finally, Tat neuropathology may be exacerbated in the presence of drugs of abuse. A number of recent reports have indicated that Tat regulation of cytokine production by astrocytes, most notably MCP-1, RANTES and IL-6, is augmented by morphine (El Hage et al., 2005, 2006).

Regardless of the well-demonstrated combined neurotoxicity of Tat and opioids in vitro, it remains unclear what may be the relationship between morphine and Tat in the setting of HIV-1 infection. Our morphine-dependent model of SIV/SHIV AIDS provides an opportunity to study the possible combined influence of Tat and morphine in vivo in the context of disease-causing viral infection. There is convincing evidence that morphine abuse leads to a more rapid disease in our model (Kumar et al., 2004). Furthermore, studies in drug-abusing populations indicated that drug abuse can contribute to enhanced neuropathogenesis. However, it remains unclear what are the effects of morphine and rapid disease on neuropathogenesis in this morphine-dependent SIV/SHIV macaque model of AIDS. This work extends our previous study on the effect of morphine and rate of disease progression on viral evolution of SIV Tat in the plasma and extends into the effects on cerebrospinal fluid evolution in the same context. As in the plasma, disease progression and extent of evolution are inversely correlated in the CSF; however, the pattern of changes indicates some differences that may indicate the effects of diverse factors in the plasma and central nervous system that drive viral evolution in the context of morphine abuse.

Results

Analysis of the evolution of the SIV17E Tat exon 1 through 20 weeks post-infection

A total of 150 independent clones were obtained for this study representing two time points (Table 1). Each clone was originally amplified from viral RNA extracted from cerebrospinal fluid samples and covered the region from 6171 to 6661 of SIV17E-Fr. For analysis, sequences were truncated to the amino acid coding region (nucleotides 6302 to 6597). We focused exclusively on Tat from SIV17E-Fr based on the same rationale as previously described (Noel and Kumar, 2006). Particularly important among these factors was that the SIV, rather than the two SHIV virus, showed the widest tissue distribution as well as the earliest and most consistent invasion into the central nervous system, within a few weeks after

Table 1
CD4+, viral load in cerebrospinal fluid and number of clones

Monkey	Sampling week [a]	$CD4^+$ T (cells/ml)	CSF viral load (10^4 copies/ml)	Number of clones [b]
Group A [c]				
1/04L	12	16	37.3	9 (5)
	18	2.9	226	10 (3)
1/28Q	14	21	1150	8 (2)
	18	6	204	9 (6)
1/42N	12	39	17.8	9 (3)
	18	10	111	8 (2)
Group B				
1/02N	14	31	0.052	10 (9)
	18	10	0.012	10 (3)
1/52N	14	707	below limit	5 (4)
	20	1365	below limit	4 (4)
1/56L	12	31	0.023	7 (1)
	20	13	0.024	5 (5)
Group C				
2/02P	12	113	0.140	9 (1)
	18	447	0.008	6 (3)
2/31P	12	334	0.008	8 (1)
	18	214	0.008	9 (9)
2/AC42	12	154	0.140	7 (1)
	18	44	0.008	17 (17)

[a] The sample was from cerebrospinal fluid from the indicated week post-inoculation.
[b] The total number of sequenced clones is shown. The number in brackets indicates the number of clones divergent from the inoculum.
[c] No Group A monkeys survived beyond week 20. 1/04L was euthanized at week 18, 1/28Q at week 20 and 1/42N at week 19.

infection. Notably, by 2 weeks post-infection, all nine monkeys in the study had detectable SIV viral RNA in the CSF. $SHIV_{KU1B}$-specific viral RNA was not found in all morphine-dependent monkeys until week 12 and was still non-detectable in the three control macaques at week 20. SHIV89.6P was not detected in any of the animals in this study by week 20 post-infection (results not shown). The total number of clones for each animal per time point is provided in Table 1 along with summaries of the CD4+ and cerebrospinal fluid viral loads for the indicated time points. Of the nine animals included in this study, six were morphine-addicted (1/04L, 1/28Q, 1/42N, 1/02N, 1/52N, and 1/56L) forming cohort 1 and three were morphine-free (2/02P, 2/31P, and 2/AC42) forming cohort 2. With respect to progression, there were three groups. Among cohort 1 animals, half progressed rapidly and maintained high viral loads and low CD4+ counts. These animals all died on or before the 20th week post-infection. These three animals, 1/04L, 1/28Q and 1/42N, form Group A: rapid progression + morphine dependence. The remaining three morphine-addicted animals showed intermediate viral loads and CD4+ counts (Group B: normal progression + morphine dependence). Finally, the three animals in cohort 2 that were not morphine-dependent (Group C: normal progression, no morphine) showed the least severe disease compared to Group A and moderately better than Group B monkeys (Table 1). The Group A, B and C designations are the same as used in a previous report of the plasma Tat evolution (Noel and Kumar, 2006).

Viral diversity and divergence are less in morphine-dependent rapid progressors and viral evolution shows less complexity

Phylogenetic analyses covering the first 20 weeks of infection showed that both diversity and divergence of the viral quasispecies, as well as the complexity of evolution were less in the context of rapid disease progression. Neighbor-joining trees (Fig. 1) indicated the least overall diversity and complexity of CSF Tat clones (open circles and triangles represent weeks 12 and 20, respectively) in Group A animals. All three rapid progressors were characterized almost exclusively by the presence of single clone branches extending from the root (SIV inoculum clone). On the other hand, clones from Groups B and C monkeys showed more extensive branching and greater complexity of evolution. This is best illustrated by 2/AC42 (Fig. 1), particularly by the 20-week time point clones; however, all six monkeys in Groups B and C show similar branching patterns which are absent among the rapid progressors.

The SIV17E-Fr Tat clones from plasma from our previous study (accession numbers: DQ007650–DQ007882; solid circles and triangles for weeks 12 and 20, respectively) were included in the trees to emphasize the greater complexity of viral evolution in the normal progressors (Noel and Kumar, 2006). Group A animals fail to form clusters for either plasma or CSF clones; however, not only do the normal progressors in Groups B and C demonstrate clustering of clones, but the plasma and CSF virus also form distinct clusters. This trend supports the notion that plasma and CSF serve as distinct compartments of virus, as has been shown for HIV (Tang et al., 2000; Strain et al., 2005). Furthermore, the early appearance of SIV in the CSF (two weeks) as compared to the late appearance of $SHIV_{KU1B}$ (12 weeks, in morphine-dependent macaques only) and absence of $SHIV_{89.6P}$ (through 20 weeks) argues in favor of virus compartmentalization between plasma and CSF and may explain the generally lower viral loads in CSF (Table 1) for each animal as compared to plasma at the same time points, reported previously (Kumar et al., 2004; Noel and Kumar, 2006).

The viral diversity, a measure of the average distance between all forms of a virus within an individual, and viral divergence, a measure of the average distance between all forms of a virus at a particular time from a unique ancestral clone, in cerebrospinal fluid are each inversely correlated to disease progression at the Tat locus (Fig. 2), as we reported previously in plasma (Noel and Kumar, 2006). The three Group A animals showed an average diversity of 0.32 ± 0.05% and divergence of 0.16 ± 0.03%. Group B animals had average diversity and divergence values 2.8-fold and 4.1-fold greater (0.89 ± 0.33%, $P < 0.05$ and 0.65 ± 0.30%, $P < 0.05$, respectively). Non-morphine controls (Group C) showed greater diversity (0.59 ± 0.24%) and divergence (0.45 ± 0.20%, $P < 0.05$) than Group A monkeys by 1.8-fold and 2.8-fold, respectively. There was no statistical difference between the diversity or divergence of Groups B and C.

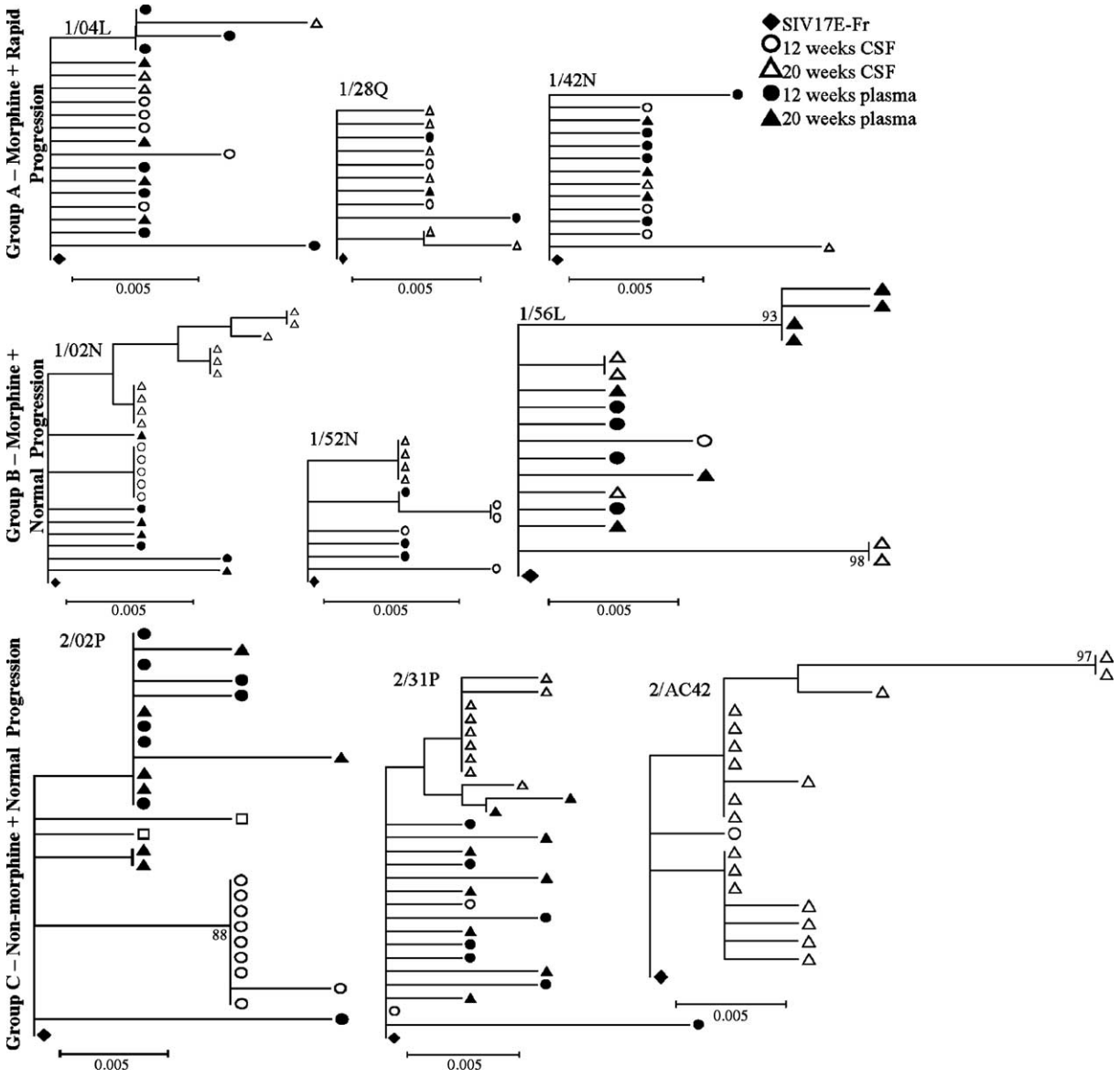

Fig. 1. Phylogenetic divergence of CSF-derived SIV Tat exon 1 clones in morphine-dependent and morphine-free SHIV/SIV-infected rhesus macaques. DNA sequences were derived from RT-PCR of cell-free viral RNA extractions of cerebrospinal fluid (open symbols) and plasma (solid symbols) at weeks 12 (circles) and 20 (triangles) post-infection. Trees were created using BioEdit (alignment) and MEGA (tree construction and editing). Clones identical to the viral inoculum (solid diamond, root of trees) were excluded to simplify the trees. Group A—morphine-dependent, rapid progressors. Group B—morphine-dependent, normal progressors. Group C—non-morphine-dependent, normal progressors. Scale bars were adjusted to represent 5 changes per 1000 nucleotides for each tree.

Morphine-dependent macaques show an altered balance of mutation type that is exacerbated by rapid disease progression

We categorized all unique (the same mutation in multiple clones from a single animal was counted only once) nucleoside substitutions as either transitions (Ts, purine to purine, pyrimidine to pyrimidine) or transversions (Tv, purine to/from pyrimidine) and compared the ratio (Ts:Tv) to assess the possible roles of morphine and/or disease progression rate on the biochemical mechanism of viral evolution. Data (Table 2) show that the Ts:Tv ratio in monkeys treated with morphine is 2.7 to 7.5 times higher, with the greatest increase in the rapid progressor group. Both increased transition and decreased transversion frequencies account for this phenomenon in the setting of morphine addiction. Transitions are nearly 15% and 23% more frequent in Group A and Group B, respectively, than in Group C. Transversions are decreased by approximately 50% in the context of morphine treatment with normal progression. Rapid disease progression exacerbates this phenomenon. Transversions in Group A animals are 70% to 85% less frequent than in Groups B and C, respectively. Interestingly, although the total diversity and divergence among the clones in Group A is statistically less than in normal progressors (Fig. 2), the total number of unique mutations occurring in all groups over the 20-week period of study was similar with 25 in Group A, 19 in Group B and 25 in Group C (Table 2). This finding is supported also by the shapes of the trees in Fig. 1, where rapid progressor clones nearly all extend from the inoculum node, while normal progressor clones show greater branching indicative of more complex evolution.

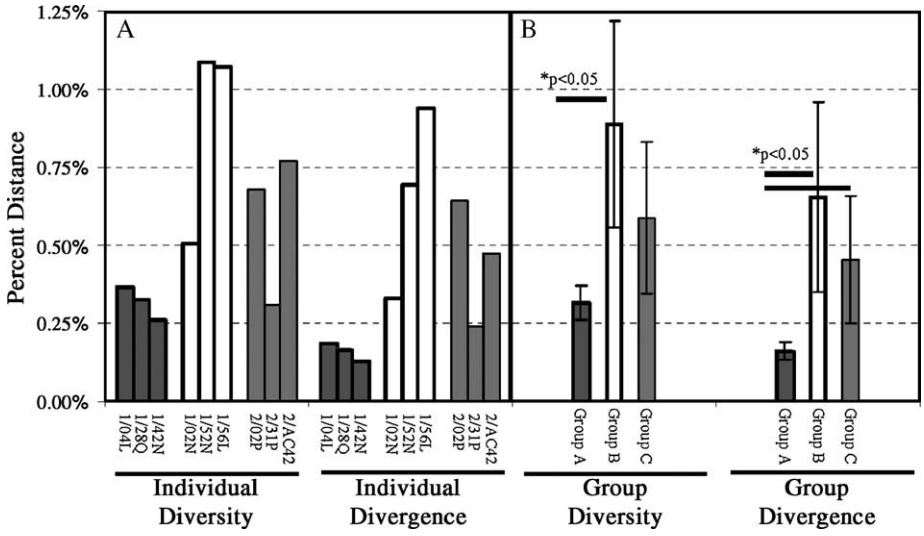

Fig. 2. Individual and group diversity and divergence. For each macaque, all sequences were aligned using BioEdit. DNADIST (part of BioEdit package) was used to calculate distance matrices. (A) Individual diversity was calculated by averaging all pairwise distances for all clones for each animal. Individual divergence values are the average of all pairwise distances from each clone to the inoculum sequence. (B) Group diversity and divergence were calculated by computing the average of the mean diversity and divergence values for each animal in each group plotted in panel A. The error bars represent the standard deviation. *P* values were found using a one-tailed, unpaired *t* test.

Neither rates of synonymous and nonsynonymous changes, nor location of nonsynonymous changes, indicate support for selective pressure; however, distinctions are evidently linked to disease progression

The sequenced clones for each animal were examined for the rates of synonymous and nonsynonymous substitution compared to the viral inoculum sequence. This analysis was done for 12-week clones, 20-week clones and all clones for each animal (Table 2). We also compared the d_S/d_N ratios to probe the potential indication of selective pressure (Lorenzo et al., 1004; Noel and Kumar, 2006; Frost et al., 2001). The group d_S/d_N ratios do not provide evidence for different selection forces among the groups (Table 2). However, the balance between synonymous and nonsynonymous changes at 12 and 20 weeks post-infection shows a different trend in Group A. Synonymous

Table 2
Summary of all unique mutations by type and frequency per non-inoculum clone

Monkey and group	Total unique mutations (Ts/Tv) [a]	Frequency per unique clone [b]	Group average and total [c]		Frequency of synonymous and nonsynonymous substitutions [d]						Monkey d_S/d_N [e]
			Frequency	Ts:Tv	17E vs. 12		17E vs. 20		17E vs. all		
					d_S	d_N	d_S	d_N	d_S	d_N	
Group A											
1/04L	11 (10/1)	Ts: 1.25, Tv: 0.13	Ts: 1.15, Tv: 0.04	24:1 (24)	0.004	0	0.005	0	0.005	0	5.46
1/28Q	8 (8/0)	Ts: 1.00, Tv: 0.00			0	0	0.004	0.001	0.002	0.001	NA
1/42N	6 (6/0)	Ts: 1.20, Tv: 0.00			0.004	0	0.003	0.001	0.003	0.001	1.79
Group B											
1/02N	4 (4/0)	Ts: 0.80, Tv: 0.00	Ts: 1.23, Tv: 0.13	17:2 (8.5)	0	0	0.013	0	0.007	0	5.06
1/52N	6 (6/0)	Ts: 1.50, Tv: 0.00			0.004	0.006	0.02	0	0.011	0.003	NA
1/56L	9 (7/2)	Ts: 1.40, Tv: 0.40			0	0.001	0.032	0	0.013	0.001	11.1
Group C											
2/02P	6 (5/1)	Ts: 1.25, Tv: 0.25	Ts: 1.01, Tv: 0.25	19:6 (3.2)	0	0.001	0	0.002	0	0.001	NA
2/31P	4 (4/0)	Ts: 0.80, Tv: 0.00			0	0	0.002	0.004	0.001	0.001	3.59
2/AC42	15 (10/5)	Ts: 1.00, Tv: 0.50			0	0	0.015	0.004	0.010	0.003	4.39

[a] The same mutation in multiple identical clones is not counted multiple times within an individual animal—even when it appears at multiple time points. The parentheses ( ) indicate the number of transition mutations, Ts, followed by the number of transversion mutations, Tv.

[b] The average number of unique mutations, by type, was calculated by dividing the number of unique mutations by the number of unique clones for each animal.

[c] Group average transition and transversion rate per unique clone is the average of the unique frequencies in the previous column. The total unique transitions and transversions for each group were tallied. A calculated Ts:Tv ratio is provided in parentheses ( ).

[d] Synonymous and nonsynonymous mutations per respective site in each clone compared only to the inoculum were tallied using SNAP (Los Alamos National Laboratories, Sequencing Database tools). 17E vs. 12 represents changes by 12 weeks, 17E vs. 20 represents changes by 20 weeks. 17E vs. all indicates all changes.

[e] The ratio was calculated for all time points compared to the inoculum clone (17E vs. all).

changes were favored in two thirds of the rapid progressors where both 1/04L and 1/42N had higher d_S than d_N, but in none of the normal progressors at 12 weeks. By 20 weeks, all animals except 2/02P favored synonymous nucleotide substitutions. This indicates that, at 12 weeks in the normally progressing animals, conditions permitted and/or favored nucleotide substitutions causing amino acid changes. Similarly, the distribution of nonsynonymous amino acid substitutions within the clones in each group is distinct based on disease progression rather than morphine abuse. Group A, B and C macaques showed a total of 16, 9 and 21 unique amino acid substitutions among all obtained clones (Fig. 3), however, only in rapid progressors were changes concentrated within the C-terminal half of Tat that contains the cysteine-rich and basic domains. In Group A, about a third of the changes (6 of 16) were within the first 50 amino acids, while the remainder occurred in the second half of the first exon. The opposite pattern occurs in the morphine-dependent normal progressors, with 2/3 of the mutations (6 of 9) in the first 50 amino acids. Group C animals show a roughly equal distribution of changes in the two halves of the first exon with 12 and 9 in the first and second halves, respectively (Fig. 3). Aside from distribution, there are no clear substitution patterns that explain the different disease outcomes. No animal showed substitutions in any of the seven critical cysteines. There were noteworthy changes in charge within the basic domain, Lys to Asp changes occurred in both 1/42N and 2/02P, but only in single clones at 18 weeks. Animals 1/04L (Group A) and 2/AC42 (Group C) had nonsense mutations in the basic region in one and seven clones, respectively. In the case of 2/AC42, this change represented the major form at 18

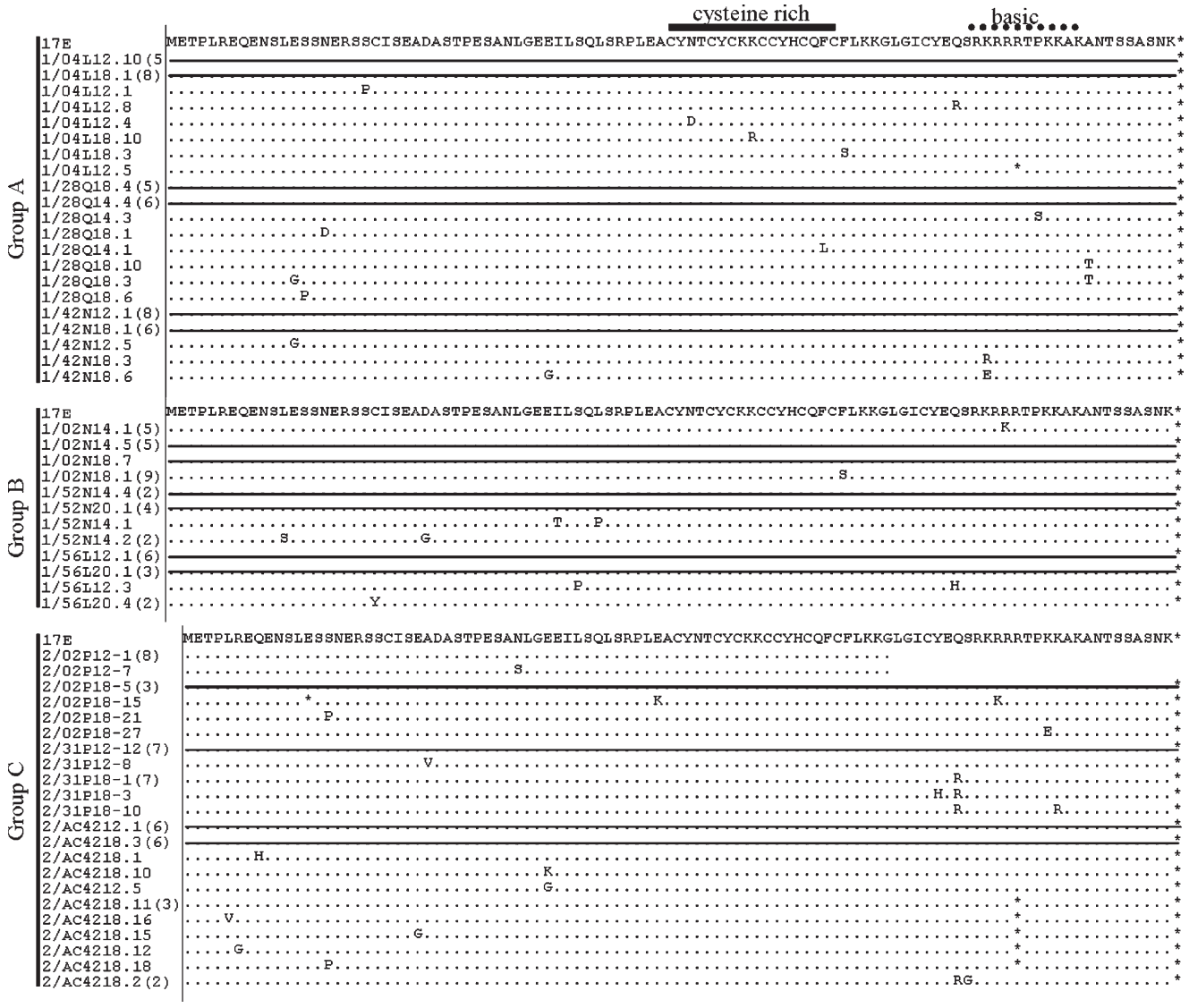

Fig. 3. Predicted protein sequences of SIV Tat exon 1. Nucleotide sequences were aligned and translated by the standard genetic code. Each unique clone per monkey per time point is shown only once; in cases where multiple identical clones were found, the number of independent isolates is indicated in parentheses ( ) next to the clone name. Sequence names (left column) indicate monkey name, week and clone number. The viral inoculum is indicated by 17E in each alignment. Clones from each monkey identical to the inoculum are indicated by a solid horizontal line. Identical positions, with respect to 17E, are indicated by a dot (.), and nonsense codons (premature truncations) are indicated by an asterisk (*). The cysteine-rich and basic domains are indicated by solid and dashed lines at the top of the figure, respectively.

weeks. However, the change did not appear in other macaques. A single clone in 2/02P at 18 weeks also showed a premature stop mutation, but only in a single clone. More interesting in 2/02P was the deletion of the final 28 amino acids in all 12-week clones (Fig. 3). However, by 18 weeks, this deletion mutant was no longer detectable, indicating a possible evolutionary dead end.

The distribution of transition mutations reflects disease progression

HIV-1 and SIV, among other retroviruses, possess a propensity toward the accumulation of G to A transition mutations. This phenomenon was reported relatively early in the epidemic for HIV (Goodenow et al., 1989; Vartanian et al., 1991, 1994) and shortly thereafter in SIV (Johnson et al., 1991; Pelletier et al., 1995). Most early explanations for the observed phenomenon were based on the high error rate of the retroviral reverse transcriptase as well as changes in the ratios of the intracellular nucleotide pools, particularly dTTP/dCTP (Martinez et al., 1994, 1995). More recently, a host restriction mechanism mediated by the APOBEC-3G/CEM15 protein has been described that offers additional explanation for the preponderance of G to A transitions known as hypermutation (Sheehy et al., 2002). We used the HYPERMUT program (Los Alamos National Laboratories) on our sequences to determine the presence and pattern of transition mutations, including any bearing G to A hypermutation signatures (Rose and Korber, 2000). Since most of our clones represented genetically intact (without nonsense codon or frameshift) sequences capable of encoding functional Tat protein variants, we do not assume that the presence of hypermutation necessitates the accumulation of defective products. This was similarly reported for small regions bearing limited changes for HIV-1 (Martinez et al., 1996). Fig. 4 shows that while all three groups exhibit G to A and non-G to A transition mutations, the patterns of transition mutation are distinct, at least with respect to disease progression. Most notably, as seen in the trees and inferred amino acid sequences (Figs. 1 and 3), the Group A animals have very few clones bearing the same transition patterns. Furthermore, only a single Group A clone, 1/04L18.10, contains multiple potential sites. On the other hand, both groups of normal progressors showed numerous clones with repeated sites of transition mutations. The existence of two or three sites was also common only to normal progressors and apparently not affected by morphine abuse.

Discussion

This study served as a follow up to our previous work showing that SIV Tat exon 1 sequence evolution in plasma was inversely related to disease progression (Noel and Kumar, 2006). Regarding sequence changes, the virus in cerebrospinal fluid showed generally the same trend as in plasma, with the rapid progressors bearing the lowest divergence from the inoculum clone and the lowest overall diversity among clones for all time points. We have also found a similar pattern of evolution of the 5′ end of SIV *env as* inversely related to progression in plasma from some of these same animals (Tirado and Kumar, 2006). However, the complexity of the evolution of the virus in CSF, particularly with respect to disease progression, was different. In plasma, we found that animals in all three groups showed more frequent evolution of clones, with nodes extending directly from the inoculum form (Noel and Kumar, 2006). That pattern of low complexity evolution was clearly evident in only the rapid progressors for CSF

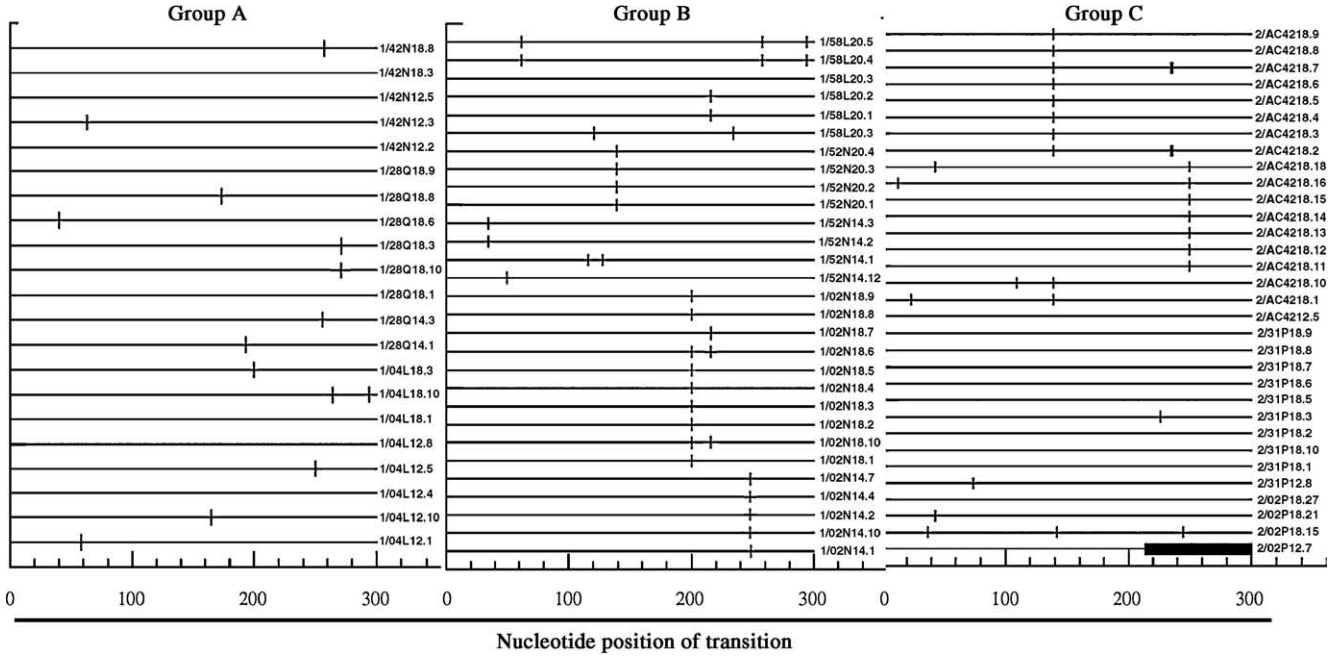

Fig. 4. Potential sites of dinucleotide and single site transition mutation. All divergent clones were analyzed using the HYPERMUT Program Package (Los Alamos National Laboratories) to identify sites of transitions and possible hypemutation among all base changes.

clones. The reason for the more extensive branching of virus in normally progressing Group B and C animals in this work is not fully clear, but it may indicate the evolution of neurotropic viral forms specific to each host as found in other viral genes during both HIV and SIV infection (Kodama et al., 1993; Gaskill et al., 2005; Strain et al., 2005). Still, this notion is difficult to reconcile with the enhanced pathogenesis in the animals with less branching as well as the known neuropathogenesis of the parent inoculum virus SIV/17E-Fr (Overholser et al., 2003; Zink et al., 1999, 2001).

Our findings showed some other interesting patterns that may indicate separate contributions of opioid abuse and disease progression rate on the mechanism of viral evolution within a host. The data demonstrate a trend of an increasing ratio of accumulation of transitions to transversions in the presence of morphine. Previous groups have reported a range of Ts:Tv ratios that can be gene-specific. While it is well described that transitions occur with a greater frequency than transversions (Moriyama et al., 1991), relatively few HIV studies have endeavored to estimate the Ts:Tv ratio that best fits their data. One study of the distribution of nonsynonymous changes that are distant in primary structure but predicted to be proximal in the tertiary structure of HIV Env found that a ratio of 6.1 was optimal (Yamaguchi-Kabata and Gojobori, 2000). An examination of evolution in nine individuals with full epidemiological information regarding transmission partners and times of transmission indicated a Ts:Tv ratio of 3.0 to 1.42 depending on viral gene (Leitner et al., 1997). None of these studies reported drug abuse as a confounding factor nor was rate of disease progression included. In our work, it appears that both morphine and disease progression may affect the balance between these two general classes of nucleotide substitutions, with morphine appearing to increase the frequency of transitions and rapid disease progression exhibiting a dramatic effect on lowering the rate of transversions among Group A clones, thus exacerbating the effect on the final ratio. We note that this trend is based on a limited number of unique mutations (Table 2) and may also be influenced by host factors, including genotype of the animals at loci known to affect viral mutation or pathogenesis, such as APOBEC3G or TRIM5α in HIV infection (Sheehy et al., 2002; Stremlau et al., 2004).

Both positive and negative selection forces have been proposed to drive HIV evolution (Wyatt and Sodroski, 1998; Yamaguchi-Kabata and Gojobori, 2000). Generally, evolution favors synonymous rather than nonsynonymous changes (Li et al., 1988); however, positive selection can drive nonsynonymous changes to expand antigenic variation (Yamaguchi-Kabata and Gojobori, 2000). In order to assess the potential for selective forces acting on the clones in this study, we examined rates of synonymous and nonsynonymous changes as well as distribution of nonsynonymous changes in the known functional domains of Tat. The functional domains for SIV Tat are not as well characterized as for HIV Tat. Still, the Tat proteins of these two lentiviruses can substitute for each other with respect to LTR transactivation (Colombini et al., 1989), thus we concentrated on two functional domains based on sequence similarities between HIV and SIV Tat: the cysteine-rich region (amino acids 50–65 of SIV Tat and 22 to 37 of HIV-1 Tat) and the basic domain (positions 80 to 90 and 49 to 57 of SIV and HIV, respectively). The cysteine-rich region has been implicated in metal binding for dimerization as well as structural integrity and in binding to host factors to stimulate transcription elongation (Hoque et al., 2003; Ruben et al., 1989; Frankel et al., 1988). This region consists of seven highly conserved cysteine residues, alteration of which results in loss of transactivation (Garcia et al., 1988; Ruben et al., 1989). The second domain is a region rich in basic amino acids that is noted for nuclear localization and in binding to the TAR loop/bulge to mediate viral transactivation (Hauber et al., 1989; Mann and Frankel, 1991; Rana and Jeang, 1999).

Additionally, positive selection may occur in regions recognized by the immune system. Notably, rhesus macaques infected with SIV have been reported to acquire CTL escape mutations at a domain within Tat bearing the sequence STPESANL, from amino acid 28 to 35 (Allen et al., 2000; O'Connor et al., 2003). The most common change is serine to proline at the first position of this motif and is detected by 14 weeks post-infection in animals of differing MHC types (O'Connor et al., 2004). This serine to proline change emerged by 12 weeks post-infection in the plasma virus of one of our control animals, 2/02P (Noel and Kumar, 2006). Interestingly, the same mutation was not discovered in 2/02P CSF clones nor in any of the other monkey CSF clones. This further supports the trend indicated in Fig. 1 that the virus in plasma and CSF represent different evolutionary compartments.

Although we do not observe preferred sites of amino acid changes among the three groups, we do find a trend of general distribution of amino acid changes that reflects disease progression rate rather than the presence of morphine. The Group A monkeys show a clear majority of nonsynonymous mutations in the C-terminal half of Tat, although without substitution of any of the essential cysteine residues. There was also a strong re-emergence of the inoculum virus, which is consistent with other reports of progressive infection (Karlsson et al., 1999), yet a substantial number of clones did arise bearing mutations among the rapid progressors as shown in Fig. 3. It is difficult to understand the cause and effect relationship of the distribution of amino acid changes and rate of progression, however, particularly in the morphine-treated animals, the differential concentration of changes in either the N or C-terminal half suggests a trend that was not apparent in our earlier work with the plasma SIV Tat sequences (Noel and Kumar, 2006). Finally, the patterns of transition mutations revealed by the HYPERMUT program (Fig. 4) lend further support to the potential relationship between disease progression rate and the biochemical mechanism of mutation in our model of morphine dependence and AIDS.

It is unclear how opiates contribute to viral pathogenesis in the CNS at the level of driving viral evolution. Our data suggest that the effects of morphine on the infected cell may alter the mutation rate and/or type of mutation that occurs. In terms of the emergence of nonsynonymous changes, it is possible that rapid disease progression is involved. We find that the distribution of amino acid changing mutations is distinct in Group A, occurring

preferentially in the C-terminus containing the functionally important cysteine-rich and basic domains. In addition, as others have reported, synonymous changes generally are favored over nonsynonymous ones. This pattern emerges quickly (by 12 weeks) only in the rapid progressors, while it is only by 20 weeks that the normally progressing macaques, regardless of the presence of morphine, show a dominance of the synonymous mutation rate. It is tempting to speculate that morphine may cause biochemical changes in the cell that promote this effect and the impact on the Ts:Tv ratio. There already exists evidence that morphine can contribute to an increase in cellular reverse transcriptase activity in SIV-infected cells (Chuang et al., 1993), which may be a sign of such a biochemically altered intracellular environment. Furthermore, a very recent study of the role of opioids in simian AIDS progression indicates that the viral mutation rate in morphine-treated animals may be subtly different (Chuang et al., 2005). This idea merits further investigation and may help to clarify the role that morphine plays in SIV/SHIV and, by analogy, HIV infection.

Methods

Animal model

A total of nine male, Indian rhesus macaques (*Macaca mulatta*) were used for these studies. At the start of morphine administration, all animals ranged in age from 1.5 to 2.5 years, weighed 3 to 4.2 kg and were free of simian T-cell leukemia virus type 1 and simian retrovirus. Animals were treated following a protocol approved by the local animal care committee (IACUC) in accordance with the *Guide for the Care and Use of Laboratory Animals*. The morphine addiction protocol has been described previously (Kumar et al., 2004; Noel and Kumar, 2006; Tirado and Kumar, 2006). Briefly, six animals (cohort 1) were made morphine-dependent over a 20-week period prior to inoculation with virus, while the remaining three macaques (cohort 2) were given saline injections during the same period to serve as controls. Cohort 1 animals were maintained at three daily intramuscular injections of morphine (each 5 mg/kg) throughout the study to avoid withdrawal effects. Infection was by intravenous route with a three-virus mixture in 2 ml containing 10^4 50% tissue culture infective doses each of simian–human immunodeficiency virus KU-1B ($SHIV_{KU\text{-}1B}$), (Singh et al., 2002), $SHIV_{89.6P}$ (Reimann et al., 1996) and SIV/17E-Fr (Flaherty et al., 1997). This combination of challenge virus results in induction of uniform disease leading to clinical AIDS in a relatively short time (Kumar et al., 2002) rather than variably over multiple years when a single virus is used (Kumar et al., 2001; Silverstein et al., 2000). During the 20-week study period following inoculation, blood and cerebrospinal fluid were collected for CBC profiles (to obtain $CD4^+$ cell counts, Table 1) and viral loads using a real time RT-PCR assay with a lower limit of sensitivity of 80 copies/ml (Amara et al., 2002), as reported previously (Kumar et al., 2004).

Amplification, cloning and sequencing of 5′ exon of tat

Viral RNA was isolated from CSF samples at the approximately 12 and 20 weeks post-infection using the QIAmp Viral RNA Mini Kit (Qiagen, Inc., Valencia, CA). In some cases, samples were from 14 or 18 weeks as dictated by CSF availability (see Table 1). Primers and PCR conditions were as reported previously. Briefly, an RT-PCR reaction was performed using the Qiagen One-Step RT-PCR kit (primers SvTat1F1 5′-GGCAGGGGGATGGAGACCAGG and SvTat1R1 5′-GCACAAAAAAGGGGAATTGTCGC) followed by a secondary PCR reaction using the Invitrogen *AccuTaq* DNA polymerase (primers SvTat1F2 5′-AAATGAAGGACCACAAAGGGAACC and SvTat1R2 5′-CCCATAGACACTTAAAAGCAAGATGGC). The 491 base pair fragment was confirmed by agarose electrophoresis prior to cloning into pPCR2.1 (Invitrogen, Carlsbad, CA). Positive clones were identified by colony screening with restriction enzyme digest (*Eco*R1, Promega) and agarose electrophoresis prior to liquid culture growth and plasmid prep using the standard protocol of the Qiagen Qiaprep Spin Mini Kit. A target of 6–10 clones per time point were sent for sequencing to the DNA Sequencing Facility of Florida State University, Department of Biological Sciences. In three cases, due to low viral loads, we acquired fewer than six clones (summarized in Table 1). Sequences of CSF clones in this study were named as in our previous study by monkey name then week then clone number; however, all names were preceded by a lowercase ‘c’ to indicate CSF origin of viral RNA. The sequences are available in GeneBank: DQ320162–DQ320311.

Sequence editing and alignment and statistics

Sequence files (*.ab1 format) were decoded and edited using BioEdit version 7.0.1 (Hall, 1999). Alignments were performed via the ClustalW algorithm with the IUB DNA weight matrix (Thompson et al., 1997) prior to truncation to the 300 bases that encode the 99 amino acid first exon. Finally, putative amino acid sequences were inferred from the nucleotide sequences using the standard genetic code. All pairwise distances for clones within each monkey (diversity) and as compared to the inoculum clone (divergence) were calculated using DNADIST (part of BioEdit program panel). Phylogenetic trees were formed using a neighbor-joining method (ClustalX) (Saitou and Nei, 1987). Group diversity and divergence were compared statistically using an unpaired, one-tailed *t* test. The statistical cut-off for significance in these analyses was $P = 0.05$.

Sequence analyses of mutation type, frequency and hypermutation

Sequence changes were assessed for potential functional changes (synonymous vs. nonsynonymous) and also based on the character of the changes (transition vs. transversion). The frequencies of synonymous (silent) changes per synonymous (d_S) site and nonsynonymous (amino acid changing) mutations per nonsynonymous site (d_N) for each clone compared to the

viral inoculum sequence were estimated using the Synonymous/Nonsynonymous Analysis Program (SNAP) from the Los Alamos National Laboratories (Nei and Gojobori, 1986). The category and rate of mutation, transition or transversion, for all point mutations were calculated from the nucleotide alignments by comparison with the inoculum. All unique mutations were tallied on the basis of type. If a base substitution occurred multiple times within a single animal at the same nucleotide position, it was counted as a single unique mutation, except in the case where a single position had multiple different substitutions. The frequency per unique clone was calculated by dividing the total number of unique transition or transversion mutations for a given animal by the total number of unique clones. The group transition to transversion ratios (Ts:Tv) were calculated by adding the total unique transition mutations in one group and dividing by the sum of the unique transversion mutations in the macaques of the same group. Potential examples of hypermutation, the excessive accumulation of transition mutations common to HIV and SIV, as well as other transition mutations were computed using the HYPERMUT program from the Los Alamos National Laboratories (Rose and Korber, 2000).

Acknowledgments

We thank Dr. Martin Hill, Department of Pharmacology, Ponce School of Medicine for insightful discussions. This work was supported by National Institute on Drug Abuse (DA015013), National Institute on Alcohol Abuse and Alcoholism (AA015045) and National Center for Research Resources (G12RR003050).

References

Abraham, S., Sawaya, B.E., Safak, M., Batuman, O., Khalili, K., Amini, S., 2003. Regulation of MCP-1 gene transcription by Smads and HIV-1 Tat in human glial cells. Virology 309, 196–202.

Allen, T.M., O'Connor, D.H., Jing, P., Dzuris, J.L., Mothe, B.R., Vogel, T.U., Dunphy, E., Liebl, M.E., Emerson, C., Wilson, N., Kunstman, K.J., Wang, X., Allison, D.B., Hughes, A.L., Desrosiers, R.C., Altman, J.D., Wolinsky, S.M., Sette, A., Watkins, D.I., 2000. Tat-specific cytotoxic T lymphocytes select for SIV escape variants during resolution of primary viraemia. Nature 21, 386–390 (Sep.).

Amara, R.R., Villinger, F., Altman, J.D., Lydy, S.L., O'Neil, S.P., Staprans, S.I., Montefiori, D.C., Xu, Y., Herndon, J.G., Wyatt, L.S., Candido, M.A., Kozyr, N.L., Earl, P.L., Smith, J.M., Ma, H.L., Grimm, B.D., Hulsey, M.L., McClure, H.M., McNicholl, J.M., Moss, B., Robinson, H.L., 2002. Control of a mucosal challenge and prevention of AIDS by a multiprotein DNA/MVA vaccine. Vaccine 20, 1949–1955.

Anderson, E., Zink, W., Xiong, H., Gendelman, H.E., 2002. HIV-1-associated dementia: a metabolic encephalopathy perpetrated by virus-infected and immune-competent mononuclear phagocytes. J. Acquired Immune Defic. Syndr. 31, S43–S54.

Bell, J.E., Brettle, R.P., Chiswick, A., Simmonds, P., 1998. HIV encephalitis, proviral load and dementia in drug users and homosexuals with AIDS. Effect of neocortical involvement. Brain 121, 2043–2052.

Chang, S.L., Moldow, R.L., House, S.D., Zadina, J.E., 1996. Morphine affects the brain-immune axis by modulating an interleukin-1 beta dependent pathway. Adv. Exp. Med. Biol. 402, 35–42.

Chang, H.C., Samaniego, F., Nair, B.C., Buonaguro, L., Ensoli, B., 1997. HIV-1 Tat protein exits from cells via a leaderless secretory pathway and binds to extracellular matrix-associated heparan sulfate proteoglycans through its basic region. AIDS 11, 1421–1431.

Chauhan, A., Turchan, J., Pocernich, C., Bruce-Keller, A., Roth, S., Butterfield, D.A., Major, E.O., Nath, A., 2003. Intracellular human immunodeficiency virus Tat expression in astrocytes promotes astrocyte survival but induces potent neurotoxicity at distant sites via axonal transport. J. Biol. Chem. 278, 13512–13519.

Chuang, L.F., Killam Jr., K.F., Chuang, R.Y., 1993. Increased replication of simian immunodeficiency virus in CEM x174 cells by morphine sulfate. Biochem. Biophys. Res. Commun. 195, 1165–1173.

Chuang, R.Y., Suzuki, S., Chuang, T.K., Miyagi, T., Chuang, L.F., Doi, R.H., 2005. Opioids and the progression of simian AIDS. Front. Biosci. 10, 1666–1677.

Colombini, S., Arya, S.K., Reitz, M.S., Jagodzinski, L., Beaver, B., Wong-Staal, F., 1989. Structure of simian immunodeficiency virus regulatory genes. Proc. Natl. Acad. Sci. U.S.A. 86, 4813–4817.

Conant, K., Ma, M., Nath, A., Major, E.O., 1996. Extracellular human immunodeficiency virus type 1 Tat protein is associated with an increase in both NF-kappa B binding and protein kinase C activity in primary human astrocytes. J. Virol. 70, 1384–1389.

Corder, E.H., Robertson, K., Lannfelt, L., Bogdanovic, N., Eggertsen, G., Wilkins, J., Hall, C., 1998. HIV-infected subjects with the E4 allele for APOE have excess dementia and peripheral neuropathy. Nat. Med. 4, 1182–1184.

Cysique, L.A., Maruff, P., Brew, B.J., 2004. Prevalence and pattern of neuropsychological impairment in human immunodeficiency virus-infected/acquired immunodeficiency syndrome (HIV/AIDS) patients across pre- and post-highly active antiretroviral therapy eras: a combined study of two cohorts. J. NeuroVirol. 10, 350–357.

Davis, L.E., Hjelle, B.L., Miller, V.E., Palmer, D.L., Llewellyn, A.L., Merlin, T.L., Young, S.A., Mills, R.G., Wachsman, W., Wiley, C.A., 1992. Early viral brain invasion in iatrogenic human immunodeficiency virus infection. Neurology 42, 1736–1739.

Donahoe, R.M., 2004. Multiple ways that drug abuse might influence AIDS progression: clues from a monkey model. J. Neuroimmunol. 147, 28–32.

Donahoe, R.M., Falek, A., 1988. Neuroimmunomodulation by opiates and other drugs of abuse: relationship to HIV infection and AIDS. Adv. Biochem. Psychopharmacol. 44, 145–158.

El Hage, N., Gurwell, J.A., Singh, I.N., Knapp, P.E., Nath, A., Hauser, K.F., 2005. Synergistic increases in intracellular Ca^{2+}, and the release of MCP-1, RANTES, and IL-6 by astrocytes treated with opiates and HIV-1 Tat. Glia 50, 91–106.

El Hage, N., Wu, G., Wang, J., Ambati, J., Knapp, P.E., Reed, J.L., Bruce-Keller, A.J., Hauser, K.F., 2006. HIV-1 Tat and opiate-induced changes in astrocytes promote chemotaxis of microglia through the expression of MCP-1 and alternative chemokines. Glia 53, 132–146.

Ensoli, B., Buonaguro, L., Barillari, G., Fiorelli, V., Gendelman, R., Morgan, R.A., Wingfield, P., Gallo, R.C., 1993. Release, uptake, and effects of extracellular human immunodeficiency virus type 1 Tat protein on cell growth and viral transactivation. J. Virol. 67, 277–287.

Flaherty, M.T., Hauer, D.A., Mankowski, J.L., Zink, M.C., Clements, J.E., 1997. Molecular and biological characterization of a neurovirulent molecular clone of simian immunodeficiency virus. J. Virol. 71, 5790–5798.

Frankel, A.D., Bredt, D.S., Pabo, C.O., 1988. Tat protein from human immunodeficiency virus forms a metal-linked dimer. Science 240, 70–73.

Frost, S.D., Gunthard, H.F., Wong, J.K., Havlir, D., Richman, D.D., Leigh Brown, A.J., 2001. Evidence for positive selection driving the evolution of HIV-1 env under potent antiviral therapy. Virology 284, 250–258.

Gabuzda, D.H., Ho, D.D., de la Monte, S.M., Hirsch, M.S., Rota, T.R., Sobel, R.A., 1986. Immunohistochemical identification of HTLV-III antigen in brains of patients with AIDS. Ann. Neurol. 20, 289–295.

Garcia, J.A., Harrich, D., Pearson, L., Mitsuyasu, R., Gaynor, R.B., 1988. Functional domains required for tat-induced transcriptional activation of the HIV-1 long terminal repeat. EMBO J. 7, 3143–3147.

Gartner, S., Markovits, P., Markovitz, D.M., Betts, R.F., Popovic, M., 1986. Virus isolation from and identification of HTLV-III/LAV-producing cells in brain tissue from a patient with AIDS. JAMA 256, 2365–2371.

Gaskill, P.J., Watry, D.D., Burdo, T.H., Fox, H.S., 2005. Development and characterization of positively selected brain-adapted SIV. Virol. J. 2, 44.

Gonda, M.A., Wong-Staal, F., Gallo, R.C., Clements, J.E., Narayan, O., Gilden, R.V., 1985. Sequence homology and morphologic similarity of HTLV-III and visna virus, a pathogenic lentivirus. Science 227, 173–177.

Gonzalez, E., Rovin, B.H., Sen, L., Cooke, G., Dhanda, R., Mummidi, S., Kulkarni, H., Bamshad, M.J., Telles, V., Anderson, S.A., Walter, E.A., Stephan, K.T., Deucher, M., Mangano, A., Bologna, R., Ahuja, S.S., Dolan, M.J., Ahuja, S.K., 2002. HIV-1 infection and AIDS dementia are influenced by a mutant MCP-1 allele linked to increased monocyte infiltration of tissues and MCP-1 levels. Proc. Natl. Acad. Sci. U.S.A. 99, 13795–13800.

Goodenow, M., Huet, T., Saurin, W., Kwok, S., Sninsky, J., Wain-Hobson, S., 1989. HIV-1 isolates are rapidly evolving quasispecies: evidence for viral mixtures and preferred nucleotide substitutions. J. Acquired Immune Defic. Syndr. 2, 344–352.

Gurwell, J.A., Nath, A., Sun, Q., Zhang, J., Martin, K.M., Chen, Y., Hauser, K.F., 2001. Synergistic neurotoxicity of opioids and human immunodeficiency virus-1 Tat protein in striatal neurons in vitro. Neuroscience 102, 555–563.

Hall, T.A., 1999. BioEdit: a user-friendly biological sequence alignment editor and analysis program for Windows 95/98/NT. Nucleic Acids Symp. 41, 95–98.

Hauber, J., Malim, M.H., Cullen, B.R., 1989. Mutational analysis of the conserved basic domain of human immunodeficiency virus tat protein. J. Virol. 63, 1181–1187.

Hollander, H., Stringari, S., 1987. Human immunodeficiency virus-associated meningitis. Clinical course and correlations. Am. J. Med. 83, 813–816.

Hoque, M., Young, T.M., Lee, C.G., Serrero, G., Mathews, M.B., Pe'ery, T., 2003. The growth factor granulin interacts with cyclin T1 and modulates P-TEFb-dependent transcription. Mol. Cell. Biol. 23, 1688–1702.

Hudson, L., Liu, J., Nath, A., Jones, M., Raghavan, R., Narayan, O., Male, D., Everall, I., 2000. Detection of the human immunodeficiency virus regulatory protein tat in CNS tissues. J. NeuroVirol. 6, 145–155.

Johnson, P.R., Hamm, T.E., Goldstein, S., Kitov, S., Hirsch, V.M., 1991. The genetic fate of molecularly cloned simian immunodeficiency virus in experimentally infected macaques. Virology 185, 217–228.

Jones, M., Olafson, K., Del Bigio, M.R., Peeling, J., Nath, A., 1998. Intraventricular injection of human immunodeficiency virus type 1 (HIV-1) tat protein causes inflammation, gliosis, apoptosis, and ventricular enlargement. J. Neuropathol. Exp. Neurol. 57, 563–570.

Kapadia, F., Vlahov, D., Donahoe, R.M., Friedland, G., 2005. The role of substance abuse in HIV disease progression: reconciling differences from laboratory and epidemiologic investigations. Clin. Infect. Dis. 41, 1027–1034.

Karlsson, A.C., Gaines, H., Sallberg, M., Lindback, S., Sonnerborg, A., 1999. Reappearance of founder virus sequence in human immunodeficiency virus type 1-infected patients. J. Virol. 73, 6191–6196.

Kim, B.O., Liu, Y., Ruan, Y., Xu, Z.C., Schantz, L., He, J.J., 2003. Neuropathologies in transgenic mice expressing human immunodeficiency virus type 1 Tat protein under the regulation of the astrocyte-specific glial fibrillary acidic protein promoter and doxycycline. Am. J. Pathol. 162, 1693–1707.

Kodama, T., Mori, K., Kawahara, T., Ringler, D.J., Desrosiers, R.C., 1993. Analysis of simian immunodeficiency virus sequence variation in tissues of rhesus macaques with simian AIDS. J. Virol. 67, 6522–6534.

Koller, H., Schaal, H., Freund, M., Garrido, S.R., von Giesen, H.J., Ott, M., Rosenbaum, C., Arendt, G., 2001. HIV-1 protein Tat reduces the glutamate-induced intracellular Ca^{2+} increase in cultured cortical astrocytes. Eur. J. Neurosci. 14, 1793–1799.

Kumar, A., Lifson, J.D., Li, Z., Jia, F., Mukherjee, S., Adany, I., Liu, Z., Piatak, M., Sheffer, D., McClure, H.M., Narayan, O., 2001. Sequential immunization of macaques with two differentially attenuated vaccines induced long-term virus-specific immune responses and conferred protection against AIDS caused by heterologous simian human immunodeficiency Virus (SHIV(89. 6)P). Virology 279, 241–256.

Kumar, A., Mukherjee, S., Shen, J., Buch, S., Li, Z., Adany, I., Liu, Z., Zhuge, W., Piatak Jr., M., Lifson, J., McClure, H., Narayan, O., 2002. Immunization of macaques with live simian human immunodeficiency virus (SHIV) vaccines conferred protection against AIDS induced by homologous and heterologous SHIVs and simian immunodeficiency virus. Virology 301, 189–205.

Kumar, R., Torres, C., Yamamura, Y., Rodriguez, I., Martinez, M., Staprans, S., Donahoe, R.M., Kraiselburd, E., Stephens, E.B., Kumar, A., 2004. Modulation by morphine of viral set point in rhesus macaques infected with simian immunodeficiency virus and simian–human immunodeficiency virus. J. Virol. 78, 11425–11428.

Kutsch, O., Oh, J., Nath, A., Benveniste, E.N., 2000. Induction of the chemokines interleukin-8 and IP-10 by human immunodeficiency virus type 1 tat in astrocytes. J. Virol. 74, 9214–9221.

Leitner, T., Kumar, S., Albert, J., 1997. Tempo and mode of nucleotide substitutions in gag and env gene fragments in human immunodeficiency virus type 1 populations with a known transmission history. J. Virol. 71, 4761–4770.

Li, W.H., Tanimura, M., Sharp, P.M., 1988. Rates and dates of divergence between AIDS virus nucleotide sequences. Mol. Biol. Evol. 5, 313–330.

Li, Y., Merrill, J.D., Mooney, K., Song, L., Wang, X., Guo, C.J., Savani, R.C., Metzger, D.S., Douglas, S.D., Ho, W.Z., 2003. Morphine enhances HIV infection of neonatal macrophages. Pediatr. Res. 54, 282–288.

Liu, X., Jana, M., Dasgupta, S., Koka, S., He, J., Wood, C., Pahan, K., 2002. Human immunodeficiency virus type 1 (HIV-1) tat induces nitric-oxide synthase in human astroglia. J. Biol. Chem. 277, 39312–39319.

Lorenzo, E., Colon, M.C., Almodovar, S., Maldonado, I.M., Gonzalez, S., Costa, S.E., Hill, M.D., Mendoza, R., Sepulveda, G., Yanagihara, R., Nerurkar, V., Kumar, R., Yamamura, Y., Scott, W.A., Kumar, A., 2004. Influence of CD4+ T cell counts on viral evolution in HIV-infected individuals undergoing suppressive HAART. Virology 330, 116–126.

Ma, M., Nath, A., 1997. Molecular determinants for cellular uptake of Tat protein of human immunodeficiency virus type 1 in brain cells. J. Virol. 71, 2495–2499.

Mann, D.A., Frankel, A.D., 1991. Endocytosis and targeting of exogenous HIV-1 Tat protein. EMBO J. 10, 1733–1739.

Martinez, M.A., Vartanian, J.P., Wain-Hobson, S., 1994. Hypermutagenesis of RNA using human immunodeficiency virus type 1 reverse transcriptase and biased dNTP concentrations. Proc. Natl. Acad. Sci. U.S.A. 91, 11787–11791.

Martinez, M.A., Sala, M., Vartanian, J.P., Wain-Hobson, S., 1995. Reverse transcriptase and substrate dependence of the RNA hypermutagenesis reaction. Nucleic Acids Res. 23, 2573–2578.

Martinez, M.A., Pezo, V., Marliere, P., Wain-Hobson, S., 1996. Exploring the functional robustness of an enzyme by in vitro evolution. EMBO J. 15, 1203–1210.

Maschke, M., Kastrup, O., Esser, S., Ross, B., Hengge, U., Hufnagel, A., 2000. Incidence and prevalence of neurological disorders associated with HIV since the introduction of highly active antiretroviral therapy (HAART). J. Neurol. Neurosurg. Psychiatry 69, 376–380.

McCoig, C., Castrejon, M.M., Castano, E., De Suman, O., Baez, C., Redondo, W., McClernon, D., Danehower, S., Lanier, E.R., Richardson, C., Keller, A., Hetherington, S., Saez-Llorens, X., Ramilo, O., 2002. Effect of combination antiretroviral therapy on cerebrospinal fluid HIV RNA, HIV resistance, and clinical manifestations of encephalopathy. J. Pediatr. 141, 36–44.

McManus, C.M., Weidenheim, K., Woodman, S.E., Nunez, J., Hesselgesser, J., Nath, A., Berman, J.W., 2000. Chemokine and chemokine-receptor expression in human glial elements: induction by the HIV protein, Tat, and chemokine autoregulation. Am. J. Pathol. 156, 1441–1453.

Moriyama, E.N., Ina, Y., Ikeo, K., Shimizu, N., Gojobori, T., 1991. Mutation pattern of human immunodeficiency virus gene. J. Mol. Evol. 32, 360–363.

Nath, A., Hauser, K.F., Wojna, V., Booze, R.M., Maragos, W., Prendergast, M., Cass, W., Turchan, J.T., 2002. Molecular basis for interactions of HIV and drugs of abuse. J. Acquired Immune Defic. Syndr. 31 (Suppl. 2), S62–S69.

Navia, B.A., Cho, E.S., Petito, C.K., Price, R.W., 1986a. The AIDS dementia complex: II. Neuropathology. Ann. Neurol. 19, 525–535.

Navia, B.A., Jordan, B.D., Price, R.W., 1986b. The AIDS dementia complex: I. Clinical features. Ann. Neurol. 19, 517–524.

Nei, M., Gojobori, T., 1986. Simple methods for estimating the numbers of synonymous and nonsynonymous nucleotide substitutions. Mol. Biol. Evol. 3, 418–426.

Neuenburg, J.K., Brodt, H.R., Herndier, B.G., Bickel, M., Bacchetti, P., Price, R.W., Grant, R.M., Schlote, W., 2002. HIV-related neuropathology, 1985 to 1999: rising prevalence of HIV encephalopathy in the era of highly active antiretroviral therapy. J. Acquired Immune. Defic. Syndr. 31, 171–177.

New, D.R., Ma, M., Epstein, L.G., Nath, A., Gelbard, H.A., 1997. Human immunodeficiency virus type 1 Tat protein induces death by apoptosis in primary human neuron cultures. J. NeuroVirol. 3, 168–173.

Nicolini, A., Ajmone-Cat, M.A., Bernardo, A., Levi, G., Minghetti, L., 2001. Human immunodeficiency virus type-1 Tat protein induces nuclear factor (NF)-kappaB activation and oxidative stress in microglial cultures by independent mechanisms. J. Neurochem. 79, 713–716.

Noel, R.J., Kumar, A., 2006. Virus replication and disease progression inversely correlate with SIVtat evolution in morphine-dependent and SIV/SHIV-infected Indian rhesus macaques. Virology 346, 127–138.

O'Connor, D.H., Mothe, B.R., Weinfurter, J.T., Fuenger, S., Rehrauer, W.M., Jing, P., Rudersdorf, R.R., Liebl, M.E., Krebs, K., Vasquez, J., Dodds, E., Loffredo, J., Martin, S., McDermott, A.B., Allen, T.M., Wang, C., Doxiadis, G.G., Montefiori, D.C., Hughes, A., Burton, D.R., Allison, D.B., Wolinsky, S.M., Bontrop, R., Picker, L.J., Watkins, D.I., 2003. Major histocompatibility complex class I alleles associated with slow simian immunodeficiency virus disease progression bind epitopes recognized by dominant acute-phase cytotoxic-T-lymphocyte responses. J. Virol. 77, 9029–9040.

O'Connor, D.H., McDermott, A.B., Krebs, K.C., Dodds, E.J., Miller, J.E., Gonzalez, E.J., Jacoby, T.J., Yant, L., Piontkivska, H., Pantophlet, R., Burton, D.R., Rehrauer, W.M., Wilson, N., Hughes, A.L., Watkins, D.I., 2004. A dominant role for CD8+-T-lymphocyte selection in simian immunodeficiency virus sequence variation. J. Virol. 78, 14012–14022.

Overholser, E.D., Coleman, G.D., Bennett, J.L., Casaday, R.J., Zink, M.C., Barber, S.A., Clements, J.E., 2003. Expression of simian immunodeficiency virus (SIV) nef in astrocytes during acute and terminal infection and requirement of nef for optimal replication of neurovirulent SIV in vitro. J. Virol. 77, 6855–6866.

Pelletier, E., Saurin, W., Cheynier, R., Letvin, N.L., Wain-Hobson, S., 1995. The tempo and mode of SIV quasispecies development in vivo calls for massive viral replication and clearance. Virology 208, 644–652.

Peterson, P.K., Sharp, B.M., Gekker, G., Portoghese, P.S., Sannerud, K., Balfour Jr., H.H., 1990. Morphine promotes the growth of HIV-1 in human peripheral blood mononuclear cell cocultures. AIDS 4, 869–873.

Peterson, P.K., Gekker, G., Hu, S., Anderson, W.R., Kravitz, F., Portoghese, P.S., Balfour Jr., H.H., Chao, C.C., 1994. Morphine amplifies HIV-1 expression in chronically infected promonocytes cocultured with human brain cells. J. Neuroimmunol. 50, 167–175.

Peterson, P.K., Gekker, G., Hu, S., Cabral, G., Lokensgard, J.R., 2004. Cannabinoids and morphine differentially affect HIV-1 expression in CD4 (+) lymphocyte and microglial cell cultures. J. Neuroimmunol. 147, 123–126.

Polazzi, E., Levi, G., Minghetti, L., 1999. Human immunodeficiency virus type 1 Tat protein stimulates inducible nitric oxide synthase expression and nitric oxide production in microglial cultures. J. Neuropathol. Exp. Neurol. 58, 825–831.

Pu, H., Tian, J., Flora, G., Woo, L.Y., Nath, A., Hennig, B., Toborek, M., 2003. HIV-1 tat protein upregulates inflammatory mediators and induces monocyte invasion into the brain. Mol. Cell. Neurosci. 24, 224–237.

Purcell, D.W., Metsch, L.R., Latka, M., Santibanez, S., Gomez, C.A., Eldred, L., Latkin, C.A., 2004. Interventions for seropositive injectors—research and evaluation: an integrated behavioral intervention with HIV-positive injection drug users to address medical care, adherence, and risk reduction. J. Acquired Immune Defic. Syndr. 37 (Suppl. 2), S110–S118.

Rana, T.M., Jeang, K.T., 1999. Biochemical and functional interactions between HIV-1 Tat protein and TAR RNA. Arch. Biochem. Biophys. 365, 175–185.

Reimann, K.A., Li, J.T., Veazey, R., Halloran, M., Park, I.W., Karlsson, G.B., Sodroski, J., Letvin, N.L., 1996. A chimeric simian/human immunodeficiency virus expressing a primary patient human immunodeficiency virus type 1 isolate env causes an AIDS-like disease after in vivo passage in rhesus monkeys. J. Virol. 70, 6922–6928.

Rose, P.P., Korber, B.T., 2000. Detecting hypermutations in viral sequences with an emphasis on G → A hypermutation. Bioinformatics 16, 400–401.

Ruben, S., Perkins, A., Purcell, R., Joung, K., Sia, R., Burghoff, R., Haseltine, W.A., Rosen, C.A., 1989. Structural and functional characterization of human immunodeficiency virus tat protein. J. Virol. 63, 1–8.

Ryan, L.A., Cotter, R.L., Zink, W.E., Gendelman, H.E., Zheng, J., 2002. Macrophages, chemokines and neuronal injury in HIV-1-associated dementia. Cell. Mol. Biol. (Noisy.-le-grand) 48, 137–150.

Saitou, N., Nei, M., 1987. The neighbor-joining method: a new method for reconstructing phylogenetic trees. Mol. Biol. Evol. 4, 406–425.

Scarpini, E., Sacilotto, G., Lazzarin, A., Geremia, L., Doronzo, R., Scarlato, G., 1991. Acute ataxia coincident with seroconversion for anti-HIV. J. Neurol. 238, 356–357.

Sheehy, A.M., Gaddis, N.C., Choi, J.D., Malim, M.H., 2002. Isolation of a human gene that inhibits HIV-1 infection and is suppressed by the viral Vif protein. Nature 418, 646–650.

Silverstein, P.S., Mackay, G.A., Mukherjee, S., Li, Z., Piatak Jr., M., Lifson, J.D., Narayan, O., Kumar, A., 2000. Pathogenic simian/human immunodeficiency virus SHIV(KU) inoculated into immunized macaques caused infection, but virus burdens progressively declined with time. J. Virol. 74, 10489–10497.

Singh, D.K., McCormick, C., Pacyniak, E., Griffin, D., Pinson, D.M., Sun, F., Berman, N.E., Stephens, E.B., 2002. Pathogenic and nef-interrupted simian–human immunodeficiency viruses traffic to the macaque CNS and cause astrocytosis early after inoculation. Virology 296, 39–51.

Squinto, S.P., Mondal, D., Block, A.L., Prakash, O., 1990. Morphine-induced transactivation of HIV-1 LTR in human neuroblastoma cells. AIDS Res. Hum. Retroviruses 6, 1163–1168.

Steele, A.D., Henderson, E.E., Rogers, T.J., 2003. Mu-opioid modulation of HIV-1 coreceptor expression and HIV-1 replication. Virology 309, 99–107.

Stoler, M.H., Eskin, T.A., Benn, S., Angerer, R.C., Angerer, L.M., 1986. Human T-cell lymphotropic virus type III infection of the central nervous system. A preliminary in situ analysis. JAMA 256, 2360–2364.

Strain, M.C., Letendre, S., Pillai, S.K., Russell, T., Ignacio, C.C., Gunthard, H.F., Good, B., Smith, D.M., Wolinsky, S.M., Furtado, M., Marquie-Beck, J., Durelle, J., Grant, I., Richman, D.D., Marcotte, T., McCutchan, J.A., Ellis, R.J., Wong, J.K., 2005. Genetic composition of human immunodeficiency virus type 1 in cerebrospinal fluid and blood without treatment and during failing antiretroviral therapy. J. Virol. 79, 1772–1788.

Stremlau, M., Owens, C.M., Perron, M.J., Kiessling, M., Autissier, P., Sodroski, J., 2004. The cytoplasmic body component TRIM5alpha restricts HIV-1 infection in Old World monkeys. Nature. 427, 848–853.

Tang, Y.W., Huong, J.T., Lloyd Jr., R.M., Spearman, P., Haas, D.W., 2000. Comparison of human immunodeficiency virus type 1 RNA sequence heterogeneity in cerebrospinal fluid and plasma. J. Clin. Microbiol. 38, 4637–4639.

Thompson, J.D., Gibson, T.J., Plewniak, F., Jeanmougin, F., Higgins, D.G., 1997. The ClustalX windows interface: flexible strategies for multiple sequence alignment aided by quality analysis tools. Nucleic Acids Res. 24, 4876–4882.

Tirado, G., Kumar, A., 2006. Evolution of SIV envelope in morphine-dependent rhesus macaques with rapid disease progression. AIDS Res. Hum. Retrovir. 22, 114–119.

Tozzi, V., Balestra, P., Lorenzini, P., Bellagamba, R., Galgani, S., Corpolongo, A., Vlassi, C., Larussa, D., Zaccarelli, M., Noto, P., Visco-Comandini, U., Giulianelli, M., Ippolito, G., Antinori, A., Narciso, P., 2005. Prevalence and risk factors for human immunodeficiency virus-associated neurocognitive impairment, 1996 to 2002: results from an urban observational cohort. J. NeuroVirol. 11, 265–273.

Turchan, J., Anderson, C., Hauser, K.F., Sun, Q., Zhang, J., Liu, Y., Wise, P.M., Kruman, I., Maragos, W., Mattson, M.P., Booze, R., Nath, A., 2001. Estrogen protects against the synergistic toxicity by HIV proteins, methamphetamine and cocaine. BMC. Neurosci. http://www. biomedcentral. com/1471-2202/2/3.

Vartanian, J.P., Meyerhans, A., Asjo, B., Wain-Hobson, S., 1991. Selection, recombination, and G–A hypermutation of human immunodeficiency virus type 1 genomes. J. Virol. 65, 1779–1788.

Vartanian, J.P., Meyerhans, A., Sala, M., Wain-Hobson, S., 1994. G → A hypermutation of the human immunodeficiency virus type 1 genome:

evidence for dCTP pool imbalance during reverse transcription. Proc. Natl. Acad. Sci. U.S.A. 91, 3092–3096.

Woodman, S.E., Benveniste, E.N., Nath, A., Berman, J.W., 1999. Human immunodeficiency virus type 1 TAT protein induces adhesion molecule expression in astrocytes. J. NeuroVirol. 5, 678–684.

Wyatt, R., Sodroski, J., 1998. The HIV-1 envelope glycoproteins: fusogens, antigens, and immunogens. Science 280, 1884–1888.

Yamaguchi-Kabata, Y., Gojobori, T., 2000. Reevaluation of amino acid variability of the human immunodeficiency virus type 1 gp120 envelope glycoprotein and prediction of new discontinuous epitopes. J. Virol. 74, 4335–4350.

Yu, X., Mao, X., Blake, A.D., Li, W.X., Chang, S.L., 2003. Morphine and endomorphins differentially regulate micro-opioid receptor mRNA in SHSY-5Y human neuroblastoma cells. J. Pharmacol. Exp. Ther. 306, 447–454.

Zhang, L., Looney, D., Taub, D., Chang, S.L., Way, D., Witte, M.H., Graves, M.C., Fiala, M., 1998. Cocaine opens the blood–brain barrier to HIV-1 invasion. J. NeuroVirol. 4, 619–626.

Zink, M.C., Suryanarayana, K., Mankowski, J.L., Shen, A., Piatak Jr., M., Spelman, J.P., Carter, D.L., Adams, R.J., Lifson, J.D., Clements, J.E., 1999. High viral load in the cerebrospinal fluid and brain correlates with severity of simian immunodeficiency virus encephalitis. J. Virol. 73, 10480–10488.

Zink, M.C., Coleman, G.D., Mankowski, J.L., Adams, R.J., Tarwater, P.M., Fox, K., Clements, J.E., 2001. Increased macrophage chemoattractant protein-1 in cerebrospinal fluid precedes and predicts simian immunodeficiency virus encephalitis. J. Infect. Dis. 184, 1015–1021.